

Graphene: A Brief Study of Its Electrical and Thermal Properties

Aenakshi Sircar

Abstract: Graphene, a semiconductor material, is being seen as a game changer in electronics. The energy band gap structure suitable for Field Effect transistor (FETs), carrier mobility, ambipolar behavior and so much more, might be a potential successor for Silicon in electronics. However, there are problems to be handled before graphene can be concluded a successor to silicon. This paper goes through the properties of Graphene that are crucial for its application in various electronics sphere and its future as a successor to silicon.

Keywords: graphene, electronics, thermal, semiconductors, lattice

1. Structure of Graphene

Graphene is a carbon allotrope in a two-dimensional structure. The honeycombed structured lattice made up of a single layer of the atom, serves as a base material for many graphite based materials [1]. The non-interacting π and π^* electrons in the two-dimensional lattice, make it easy for conducting different physical and chemical processes on the surface of the graphene [2]. Due to its ideal 2D structure, Graphene exhibits properties like the Dirac Fermion which lead to the Quantum Hall Effect [3], it possesses high thermal conductivity of about $\sim 4000 \text{ Wm}^{-1}\text{K}^{-1}$ and has massless low energy excitation. Graphene also has the ability to easily convert electrical energy to heat, because of the high Seebeck's coefficient [4].

The valance band formed by the π electron and the conduction band by the π^* touch each other at a point known as the Dirac point also called the point of neutrality which consists of six points of contact between the two bands. The band structure of Graphene can be visualized as two cones because of the linear dispersion of the bands. The two cones touching each other at the E_{dirac} point as shown in Fig (1c) and (1d). The zero-band gap between the valance and the conducting band is indicated by the touching cones [4].

in 3D (c) Linear dispersion of the bands (d) Dirac Point, created by the approximate low energy band structure. [4] In Figure (1b), the six points of contact form two independent pairs called the K and K' due to symmetry of the lattice.

1.1. Graphene Lattice and the Dirac Point

As stated before, Graphene is a Honeycomb Lattice, with two carbon atoms per unit cell, where the distance between the two carbon atom is about 1.42 \AA . They together form a kind of a hexagonal structure. The lattice can be expressed using the unit vectors like:

$$\alpha_1 = \frac{a}{2}(3, \sqrt{3}), \alpha_2 = \frac{a}{2}(3, -\sqrt{3}) \quad \dots \dots \text{eq}(1)$$

The position of K and K' in space are given by the following

$$K = \left(\frac{2\pi}{3a}, \frac{2\pi}{3\sqrt{3}a} \right), K' = \left(\frac{2\pi}{3a}, -\frac{2\pi}{3\sqrt{3}a} \right) \dots \dots \text{eq}(2)$$

Density Functional Theory and Graphene Simulation is often employed to predict the electronic structure of graphene [5].

2. Properties of Graphene

2.1 Ambipolar Electric Field Effect

The carrier transportation properties of Graphene are enhanced largely in an ambipolar electric field effect. The concentration of holes and electrons n can change continuously with a value of about 10^{13} cm^{-2} [6]. The mobility μ of the speed carriers can go upto $15000 \text{ cm}^2\text{V}^{-1}\text{s}^{-1}$. The effect of Ambipolar Electric field on single layer Graphene can be clearly seen in the Figure 2.

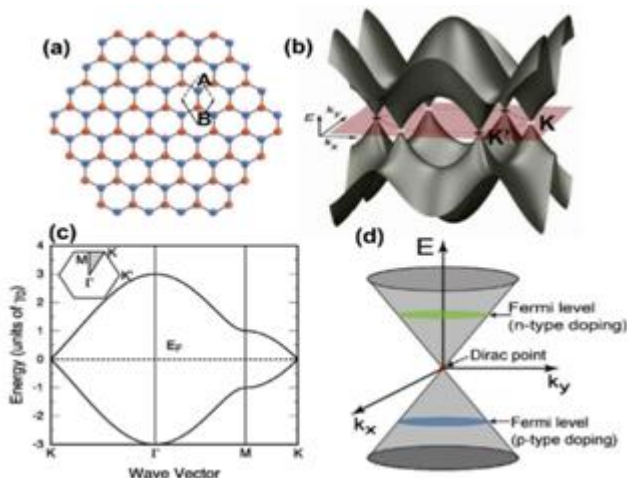


Figure 1: (a) Two atoms per unit cell of Graphene (b) The six point where the valance and the conduction band touch, shown

Volume 11 Issue 10, October 2022

www.ijsr.net

Licensed Under Creative Commons Attribution CC BY

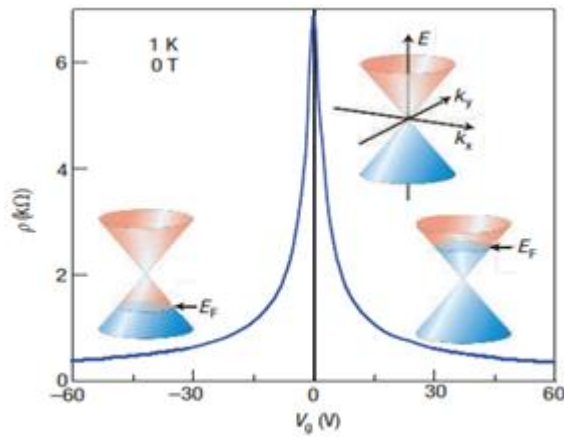


Figure 2: The effect of Ambipolar Electric Field on single-layer graphene

In Figure 2, E_F marked on the cones in the inset shows the changing Fermi Level on changing the gate voltage V_g of Graphene.

2.2. Quantum Hall Effect (QHE)

Graphene’s strong electronic properties are further proved by its ability to exhibit the Quantum Hall Effect, even at room temperature. The QHE temperature range for graphene is 10 times larger than other two-dimensional materials [6]. The Shubnikov de Haas Oscillations progress towards the QHE when fermions that are massless in nature are made to react in a magnetic field. This reaction becomes more apparent when it takes place in the high field limit.

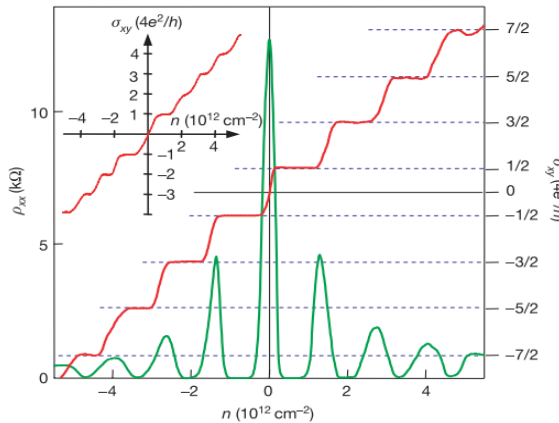


Figure 3: The graph depicts the Hall Conductivity (red), and longitudinal resistivity (green) of graphene vs the carrier concentration [7].

In Figure 3, the Hall Conductivity (red) = σ_{xy} , and Longitudinal resistivity (green) = ρ_{xx} is shown with the carrier concentration n in the presence of a constant magnetic field $B=14T$ and temperature $4K$. The progression of the plateaus for the Hall Effect curve was expected to be

$$\sigma_{xy} = (4e^2/h)N \dots \dots eq(3)$$

Where N is an integer

As shown in Fig 4, the QHE in bilayer Graphene for massive Dirac Fermion is very precise, such that the Hall Conductivity σ_{xy} , when undoped, progresses with a plateau at all values of integer N given in equation number (3), except at $N=0$. The progression misses a plateau at $N=0$, as indicated by the red arrow. However, the plateau at $N=0$ resurfaces when the graphene is doped [6].

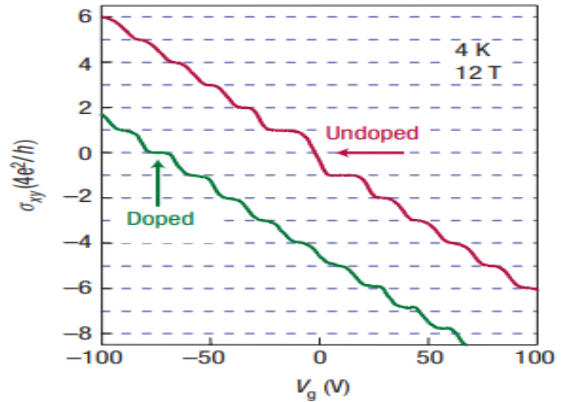


Figure 4: The unconventional Quantum Hall Effect on Bilayer Graphene for massive Dirac Fermions [6].

As in Fig 3. The quantum Hall Effect progresses and goes on like a ladder that continues to go through the Dirac point where the electrons and the holes exchange. If this QHE sequence is shifted by half, such that

$$\sigma_{xy} = (4e^2/h)(N + \frac{1}{2}) \dots \dots eq(4)$$

Where N is the Landau Level or the lowest electron level. This shift is also known as the ‘half-integer’ QHE sequence [6]. The unconventional QHE sequence is a result of the presence of a quantized level at the zero energy level in Fig. 5(1). Coupling of pseudospin and orbital motion can also account for the half integer QHE sequence. This results in a phenomena termed as the Berry’s Phase. Massive Dirac Fermions too have a pseudospin associated to them which is not clearly observable when $N \gg 1$. However, it reappears when the zero-Energy Landau level degenerates in Fig 5(2).

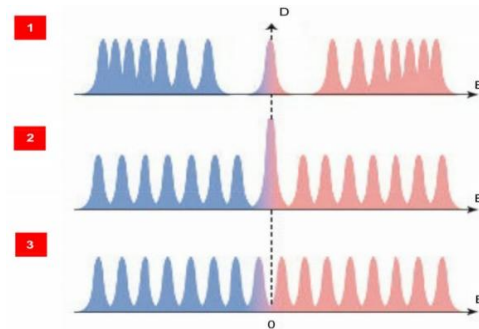


Figure 5: Types of Landau quantization in Graphene [6].

The electric field effect is used to recover the standard QHE in bilayered graphene. A certain amount of gate voltage has to be applied to bring about this change. This additional gate voltage not only changes the carrier concentration but also creates a semiconductor gap caused due to the asymmetry between the two layers of graphene. This semiconductor gap is functional in eliminating the unnecessary degeneracy of the zero-E Landau level, resulting in the continuous QHE sequence by splitting the double step as shown in Fig 5(3). [8-9]. However, the splitting can be observed only when the Dirac point is examined at a finite gate voltage, which is usually achieved with additional doping [9].

2.3 Carrier Transport in Graphene

The transport speed of carriers in ballistic regimes of Graphene can have a Fermi velocity up to $v_F \approx 10^6 \text{ ms}^{-1}$. The density of carriers is an essential factor affecting the carrier's mobility in the graphene lattice. In an instance, where the interaction between the substrate and graphene is eliminated, that is exfoliated, suspended graphene (SG), the carrier mobility of about $200000 \text{ cm}^2 \text{ V}^{-1} \text{ s}^{-1}$ has been observed [10]. This speed is almost 10 times higher than that obtained in the case of Indium Phosphide.

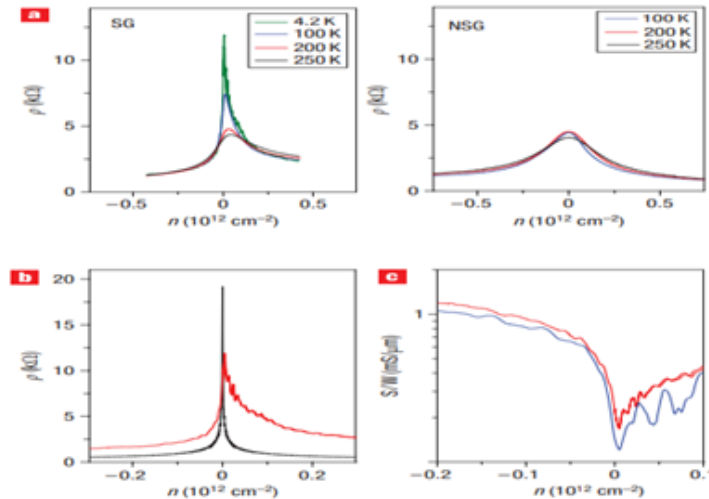


Figure 6: Dependence of carrier transport on carrier density [10]

(a). Resistivity vs carrier concentration of a suspended graphene device, at different temperatures with a channel length and width of $0.5\mu\text{m}$ and $1.4\mu\text{m}$. The resistivity vs carrier concentration graph of a Non-Suspended Graphene(NSG) device is shown on the right panel. The peak value of resistivity almost corresponds to the point of neutrality of the NSG. This shows the presence of extrinsic doping.(b). Superimposing Figure (6a) on the left panel, with the ballistic model prediction (in black) at temperature $T=0$.(c). Conductance per unit width of two suspended devices of different dimensions. The device with the red curve has a length of $0.5\mu\text{m}$ and width of $1.4\mu\text{m}$ and the device with the blue curve has a length of $0.25 \mu\text{m}$ and width of $0.9 \mu\text{m}$, both at 4.2K temperature.

Although graphene is not suited for digital switching applications, it is still a material of great interest because of its excellent carrier mobility, stability, transconductance, and thin structure of it. These properties indicate that it might possess the capability to make ideal RF electronics device [2]. The

Density of State (DOS) and the Fermi energy are instrumental in controlling the switching action in a Graphene device.

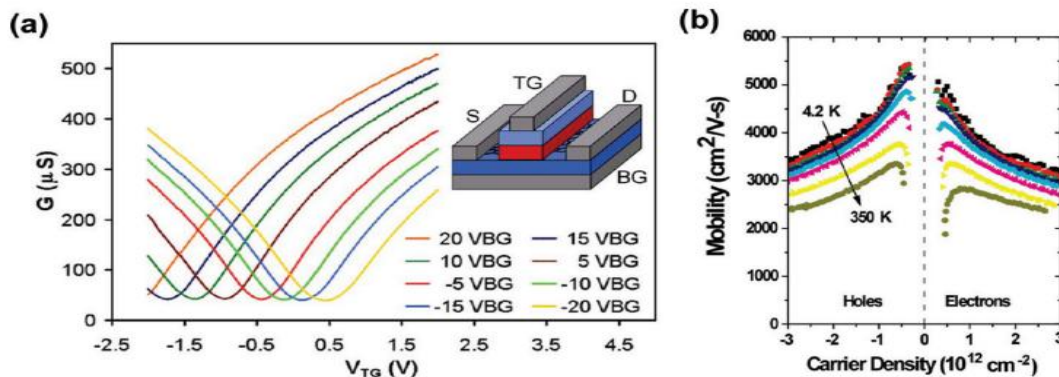


Figure 7: (a). Variation in conductance of graphene devices due to different back gate voltages as a function of a top gate biased voltage. Inset: Structure of the device having stacked gates made out of polystyrene (NFC) and HfO_2

(b). Graph of Carrier mobilities vs. Carrier Density of a transistor channel made out of single layer, exfoliated graphene, at different temperature based on Hall effect. [11-12]

2.4 Optical Properties of Graphene

Taking k-conservation, that is, observing transition only along the vertical axis, then using the Fresnel equation, we can derive the light transmittance through a thin graphene film as [13]:

$$T = (1 + \frac{\pi\alpha}{2})^{-2} \approx 1 - \pi\alpha \approx 0.977 \dots\dots eq(5)$$

Where T is the light transmittance, α is the constant of the fine structure. The result of this equation indicates that, graphene

could transmit about 97.7 percent of the incident light and absorb the remaining 2.3 percent of it [13-14]. Slight deviations were observed for far IR and UV the amount of light absorbed can be controlled by the amount of external gate voltage applied on the graphene film [15]. The excellent light transmission and conductivity of graphene makes it a great conductive electrode, which can have several applications such as OLEDs, flat panel displays, solar cells etc [16].

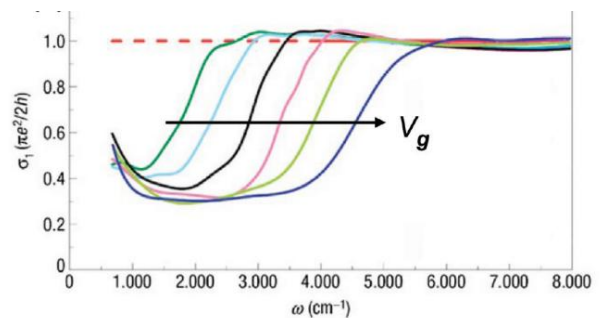
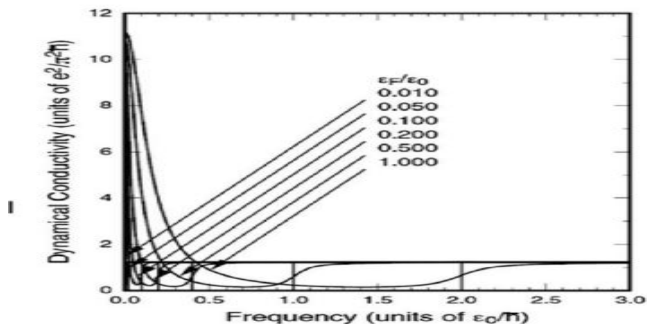


Figure 8: (a). The graph shows a theoretically predicted changes in optical absorption due to changes in the applied EF voltage. [15] (b). Shifts in the absorption of infrared light of a monolayer graphene due to gate biasing, that is used for doping the film [2, 15]

The non linear optical properties of graphene are also important properties that can be used in certain devices such ultra short pulse laser. Since this device is based on mode-locking, it employs a non linear device called the saturable absorber which produces a train of ultra short light pulses from the output of the laser. The output of the laser is a continuous wave. As of today’s time, semiconductor saturable devices are used for the purpose of mode locking, but they have small tuning range and is difficult to fabricate. Whereas graphene with its large absorption range, can put to better use for the same [17].

2.5 Thermal Conductivity of Graphene

The Fourier Law of thermal conduction says that,

$$q = -K\Delta T \dots\dots eq(6)$$

Where, q is the heat flux per unit area, K is the thermal conductivity and ΔT is the difference in temperature [18]. The specific heat capacity (C) of a material is amount of heat absorbed per unit mass with per unit change in temperature. It is composed of the lattice vibrations or phonons and negatively charged particles or the electrons. In graphene, however, the phonon plays the major role in specific heat of it, at all temperatures [19].

As shown in Fig.9, the phonon specific heat increases as the temperature rises [20-21].

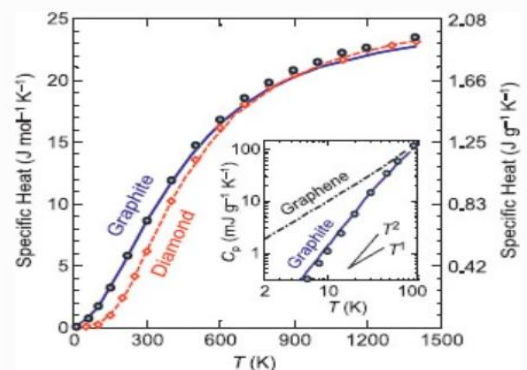


Figure 9: The specific heat capacity of graphite, diamond and graphene. In all of them Phonon plays the major role in temperature above 1 Kelvin. Inset: Specific heat capacity of graphene at low temperature is higher than graphite because of the involvement of low frequency phonon [20].

There exists a relation between thermal conductivity and the specific heat, such as

$$K \approx Cv\lambda \dots\dots eq(7)$$

C is the specific heat capacity, v is the average phonon group velocity and λ is the mean free path. From the equation (6), it can be clearly concluded that the thermal conductivity is

dependent on the specific heat capacity, and the specific heat capacity is dependent on the phonon activity. Thus, as a consequence the thermal conductivity of graphene is also heavily influenced by phonon activity.

2.6 Thermoelectric Properties of Graphene

The efficiency of a thermo electric material is indicated by the thermo- electric figure of merit, which is given by [22]:

$$ZT = T\sigma S^2 / K \quad \dots\dots eq(8)$$

ZT = Thermo Electric Figure of Merit.

σ = Electrical Conductivity.

S = Seebeck's Coefficient.

T = Absolute Temperature Coefficient.

K = Thermal Conductivity

As mentioned earlier, the thermal conductivity of a material is composed of the lattice vibrations or phonons and electrons [23]. Thus,

$$K = K_{ph} + K_e \quad \dots\dots eq(9)$$

Graphene nanostructure can be instrumental in aiding various kind of thermoelectric research and application. Some research shows that graphene nanostructure has the ability to naturally combine the following two concepts. First, given by Hicks and Dresselhaus in 1993 which says that decreasing the dimensions can improve ZT [24]. And, the second one, which found that nanostructuring can increase the ZT of a material [22].

Graphene is also capable of delivering large amount of thermoelectric power (TEP), as indicated by few experiments. At the TEP of graphene can be about ~ 50 to $100 \mu\text{V K}^{-1}$ and at room temperature about $80 \mu\text{V K}^{-1}$ [25].

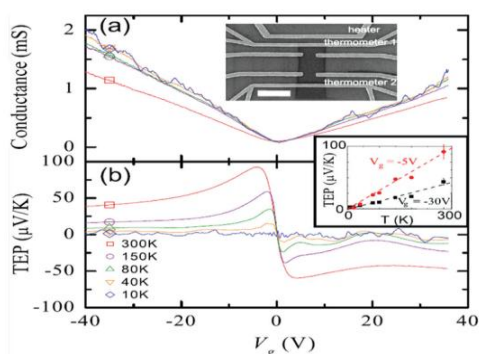


Figure 10: (a) Electrical Conductance of a graphene sample (b) TEP of a graphene sample given as a function of back gate voltage at different temperature values. Lower inset: TEP of graphene at gate voltages -30 V (black curve) and -5V (red curve)

The Seebeck's coefficient for graphene also varies with temperatures, the values varying from ~ 100 to $\sim 10 \mu\text{V K}^{-1}$ for temperatures ranging from ~ 100 to $\sim 300\text{ K}$ as shown in

Fig.11 [26]. Although graphene has a high value of the Seebeck's coefficient as compared to other semiconductor materials.

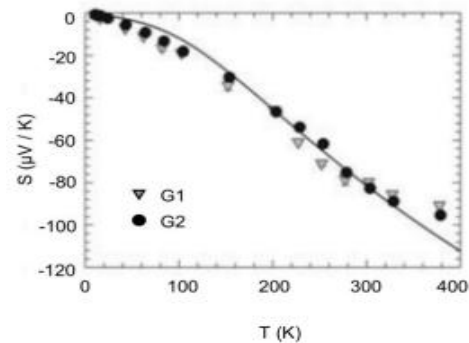


Figure 11: Variation in the Value of the Seebeck's Coefficient as a function of temperature for two different samples of graphene [26]

3. Conclusion

Graphene is one of the most researched materials in recent years. Its exceptional physical properties make it a very viable successor to silicon and possibly replace it in many semiconductor-based devices in the near future. The structure of graphene, its low atomic mass, and small dimension, give it a high thermal conductivity. This property can be exploited even more extensively in the near future. Various research have contributed to the knowledge about graphene's property which can find its application in various optical devices, electric, thermal, biothermal sensors and many other applications. Its high thermoelectrical power can be used in energy harvesting applications. This paper explores the properties of graphene which might have the capacity to replace silicon in the near future.

References

- [1] Sang, M., Shin, J., Kim, K. and Yu, K.J., 2019. Electronic and thermal properties of graphene and recent advances in graphene based electronics applications. *Nanomaterials*, 9(3), p.374.
- [2] Avouris, P., 2010. Graphene: electronic and photonic properties and devices. *Nano letters*, 10(11), pp.4285-4294.
- [3] Novoselov, K.S.; Geim, A.K.; Morozov, S.V.; Jiang, D.; Katsnelson, M.I.; Grigorieva, I.V.; Dubonos, S.V.; Firsov, A.A. Two-dimensional gas of massless dirac fermions in graphene. *Nature* 2005, 438, 197
- [4] Seol, J.H.; Jo, I.; Moore, A.L.; Lindsay, L.; Aitken, Z.H.; Pettes, M.T.; Li, X.; Yao, Z.; Huang, R.; Broido, D.; et al. Two-dimensional phonon transport in supported graphene. *Science* 2010, 328, 213–216.
- [5] Chan, K.T.; Neaton, J.B.; Cohen, M.L. First-principles study of metal adatom adsorption on graphene. *Phys. Rev. B* 2008, 77, 235430.

- [6] Geim, A.K.; Novoselov, K.S. The rise of graphene. *Nat. Mater.* 2007, 6, 183.
- [7] Novoselov, K.S.; Geim, A.K.; Morozov, S.V.; Jiang, D.; Katsnelson, M.I.; Grigorieva, I.V.; Dubonos, S.V.; Firsov, A.A. Two-dimensional gas of massless dirac fermions in graphene. *Nature* 2005, 438, 197.
- [8] McCann, E. Asymmetry gap in the electronic band structure of bilayer graphene. *Phys. Rev. B* 74, 161403 (2006).
- [9] Castro, E. V. et al. Biased bilayer graphene: semiconductor with a gap tunable by electric field effect. Preprint at <http://arxiv.org/abs/cond-mat/0611342> (2006).
- [10] X. Du, X.; Skachko, I.; Barker, A.; Andrei, E. Y. *Nat. Nanotechnol.* 2008, 3, 491.
- [11] Farmer, D. B.; Chiu, H.-Y.; Lin, Y.-M.; Jenkins, K.; Xia, F.; Avouris, Ph. *Nano Lett.* 2009, 9, 4474
- [12] Zhu, W., Perebeinos, V., Freitag, M. and Avouris, P., 2009. Carrier scattering, mobilities, and electrostatic potential in monolayer, bilayer, and trilayer graphene. *Physical Review B*, 80(23), p.235402.
- [13] Ando, T., Zheng, Y. and Suzuura, H., 2002. Dynamical conductivity and zero-mode anomaly in honeycomb lattices. *Journal of the Physical Society of Japan*, 71(5), pp.1318-1324
- [14] Kuzmenko, A. B.; van Heumen, E.; Carbone, F.; van der Marel, D. *Phys. Rev. Lett.* 2008, 100, 117401.
- [15] Li, Z., Henriksen, E., Jiang, Z. et al. Dirac charge dynamics in graphene by infrared spectroscopy. *Nature Phys* 4, 532–535 (2008).
- [16] Ahn, J. H.; Hong, B. H.; et al. *Nat. Nanotechnol.* Published on line June 20, 2010.
- [17] Sun, Z., Hasan, T., Torrisi, F., Popa, D., Privitera, G., Wang, F., Bonaccorso, F., Basko, D.M. and Ferrari, A.C., 2010. Graphene mode-locked ultrafast laser. *ACS nano*, 4(2), pp.803-810.
- [18] Bonetto, F.; Lebowitz, J.L.; Rey-Bellet, L. Fourier's law: A challenge to theorists. *Math. Phys.* 2000, 128–150.
- [19] Benedict, L.X.; Louie, S.G.; Cohen, M.L. Heat capacity of carbon nanotubes. *Solid State Commun.* 1996, 100, 177–180.
- [20] Pop, E.; Varshney, V.; Roy, A.K. Thermal properties of graphene: Fundamentals and applications. *MRS Bull.* 2012, 37, 1273–1281.
- [21] Yi, W.; Lu, L.; Dian-lin, Z.; Pan, Z.W.; Xie, S.S. Linear specific heat of carbon nanotubes. *Phys. Rev. B* 1999, 59, R9015–R9018.
- [22] Xu, Y., Li, Z. and Duan, W., 2014. Thermal and thermoelectric properties of graphene. *Small*, 10(11), pp.2182-2199.
- [23] Kim, H.S.; Liu, W.; Chen, G.; Chu, C.-W.; Ren, Z. Relationship between thermoelectric figure of merit and energy conversion efficiency. *Proc. Natl. Acad. Sci. USA* 2015, 112, 8205–8210.
- [24] L. Hicks, M. Dresselhaus, *Phys. Rev. B* 1993, 47, 12727.
- [25] Wei, P.; Bao, W.; Pu, Y.; Lau, C.N.; Shi, J. Anomalous thermoelectric transport of dirac particles in graphene. *Phys. Rev. Lett.* 2009, 102, 166808.
- [26] Seol, J.H.; Jo, I.; Moore, A.L.; Lindsay, L.; Aitken, Z.H.; Pettes, M.T.; Li, X.; Yao, Z.; Huang, R.; Broido, D.; et al. Two-dimensional phonon transport in supported graphene. *Science* 2010, 328, 213–216.